Supplementary figure and movie legends for:

# Vibrissa-based object localization in head-fixed mice

**Daniel H. O'Connor, Nathan G. Clack, Daniel Huber, Takaki Komiyama, Eugene W. Myers, Karel Svoboda**

Janelia Farm Research Campus, HHMI, 19700 Helix Drive, Ashburn, VA 20147

SUPPLEMENTARY FIGURE 1: Line detector used for tracing whisker segments.

**A**, The line detector consists of two step-edge detectors with the same orientation, positioned relative to a pixel anchor with a sub-pixel displacement (offset). **B**, Pixilated representation of a line detector. The value of each pixel is the integral of the detector over the pixel area.

SUPPLEMENTARY FIGURE 2: Learning curves for mice trained under "worst-case" circumstances.

**A**, Learning curves for a cohort of six mice in which training was interrupted by a gap of about a month, and in which mice were moved among different training rigs. Each data point shows performance averaged over a session. Hollow data points indicate the first-stage of training in which go and no-go stimuli were separated by D = 8.57 mm (see Materials and Methods). Solid points indicate an easy version of the final task in which stimuli are separated by D = 4.29 mm. Dashed lines indicate 90% and 50% correct performance. Prior to the first data point mice had 1-2 sessions (~10-15 min each) of learning to lick at the lickport. After the sessions indicated by arrows, there was a gap of 34-35 days during which the mice were not trained. **B**, Cumulative

histogram of the number of daily localization sessions to an 85% correct performance criterion across mice. The fastest mouse achieved criterion performance in 11 sessions, the slowest in 18 sessions.

SUPPLEMENTARY FIGURE 3: Cortex aspiration lesions.

Cytochrome oxidase-stained coronal sections through the brain of one mouse used for contralateral-side somatosensory cortex lesions (top) and one mouse with a lesion ipsilateral to the stimulus (bottom). L, left hemisphere.

SUPPLEMENTARY FIGURE 4: Order of sessions for psychometric curves.

Panels for each mouse show the order in which localizations of different difficulties (offsets, D) were presented during acquisition of the psychometric curves. Sessions at the different difficulties were roughly counterbalanced, with the exception of the most difficult offset (D = 0.48 mm), tested in two mice.

SUPPLEMENTARY FIGURE 5: Examples of whisking search strategies for multiple consecutive trials.

Movie-style projections of three tracked whiskers (D4, green; D3, red; D2, blue) through time in consecutive 100 ms bins, for 28 go trials (left) and 28 no-go trials (right). Each row of projections depicts a single trial. Anterior is at top. Each 100 ms bin is the projection of whiskers through 50 frames (acquired at 500 Hz) and shows the region of space explored within that 100 ms period. There are 11 bins covering the period from 0 to 1.1 sec, arranged left to right. The light gray slanted bar at top indicates approximate travel time of the pole on its

descent. The dark gray horizontal bar indicates that the pole is in its bottom position. Trials are from a single behavioral session and are in order of consecutive presentation (although sorted into go and no-go), with trial number increasing along rows from top to bottom. Solid black circles depict the pole location. Dashed black circles indicate the position of the pole on the other type of trial. Gray fill in the circles indicate that the pole is at the bottom of its range and within reach of the whiskers in that time bin. The vertical black box indicates the bin containing the mean reaction time. Movies give a sense of the variability and stereotypy from trial to trial. On go trials, the whiskers are sometimes in motion during the early bins, before the pole is in reach, and sometimes start moving only later. In many trials the mouse has positioned at least one of its whiskers in the path of the go-stimulus, in a position more protracted than the resting position of the whiskers (which is not shown). After initial contact with the go stimulus, the mouse pressed D4 (green) against the pole for hundreds of milliseconds before protracting past the pole (toward the top of each image) in order to make a lick response. On no-go trials, again the mouse sometimes moves its whiskers prior to the time at which the pole is in reach and sometimes not. After the pole is in reach, the whiskers explore the go position even though the pole is in the no-go position. In a small number of trials, the mouse has positioned a whisker in the path of the go stimulus and makes few whisker movements; in this case lack of contact identifies the trial as a no-go. On no-go trials there is no systematic protraction of D4 in later bins because the mouse withholds a response instead of moving forward to lick. Performance for the trials shown was 96% correct. Six of the eight trials shown in Fig. 10 are included here (Fig. 10A,C,D).

SUPPLEMENTARY FIGURE 6: Examples of high-velocity whisker movements from a single behavioral session.

**A,** Two examples of slip-induced high velocities. Each row shows images from a single trial. In each trial, whisker D4 sticks against and then slips past the pole, achieving a velocity of ~7000 deg/sec (top row) or ~5000 deg/sec (bottom row). Ringing of the whisker after the slip appears as a motion-induced blur accompanied by no overall change in position. **B**, Two examples of purely self-generated (that is, without slip) high velocities. Each row shows images from a single trial. Both trials are from the same behavioral session as in **A**. In each trial, whisker D4 rapidly retracts, achieving velocities of ~-1214 deg/sec (top row) and ~-1438 deg/sec (bottom row). In general, the highest velocities were seen following stick-slip events.

SUPPLEMENTARY MOVIE 1: Mouse JF4004 performing an easy (D = 4.29 mm) object localization.

Example movie of a head-fixed mouse performing absolute object localization at an easy offset of D = 4.29 mm (~23.6° of azimuth).

SUPPLEMENTARY MOVIE 2: Mouse JF4004 performing a medium-difficulty (D = 2.38 mm) object localization.

Example of a head-fixed mouse performing absolute object localization at a middle-difficulty offset of D = 2.38 mm (~13.7° of azimuth). Same mouse as Supplementary Movie 1 but from a different session.

SUPPLEMENTARY MOVIE 3: Mouse JF4004 performing a difficult (D = 0.95 mm) object localization.

Example of a head-fixed mouse performing absolute object localization at a difficult offset of D = 0.95 mm (~5.6° of azimuth). In the group of trials shown, the mouse gets all trials correct except the last. However, average performance is less good (see Figure 7A). The last trial is a false alarm and the airpuff plus timeout punishment is shown. Same mouse as Supplementary Movies 1-2 but from a different session.

SUPPLEMENTARY MOVIE 4: Tracking whiskers in high-speed video of head-fixed mice.

Example of tracking whiskers in a head-fixed mouse in our experimental apparatus. Left panel shows high-speed video with tracked whiskers indicated in different colors. Top right panel shows azimuthal angle ($\theta$) computed from the tracked whiskers (indicated with matching colors). Bottom right panel shows for one whisker (magenta, D2) change in curvature ($\Delta$curvature; curvature minus the mean curvature over the first 100 ms of the video) as a function of $\theta$. Note the signature trajectory in this space associated with whisker contact. The video was recorded at 500 frames/sec and is played back at 15 frames/sec.

Supplementary Fig 1: Line detector used for tracing whisker segments.

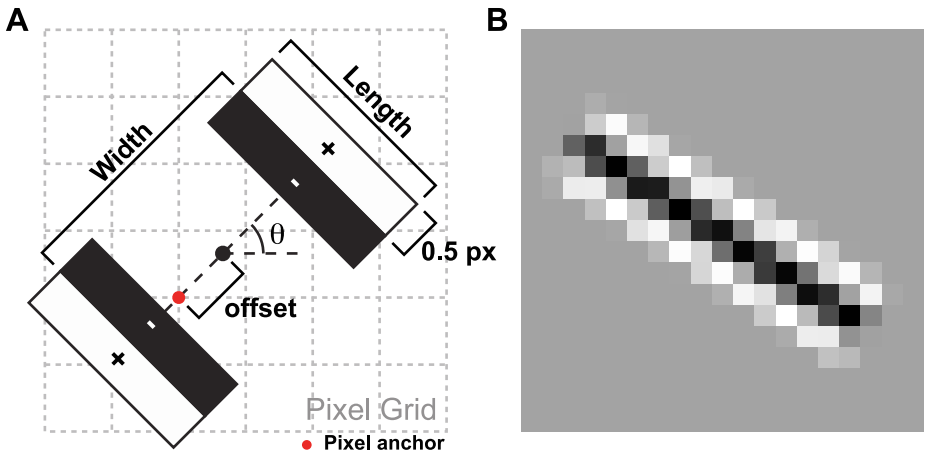

Supplementary Fig 2: Learning curves for mice trained under "worst case" circumstances.

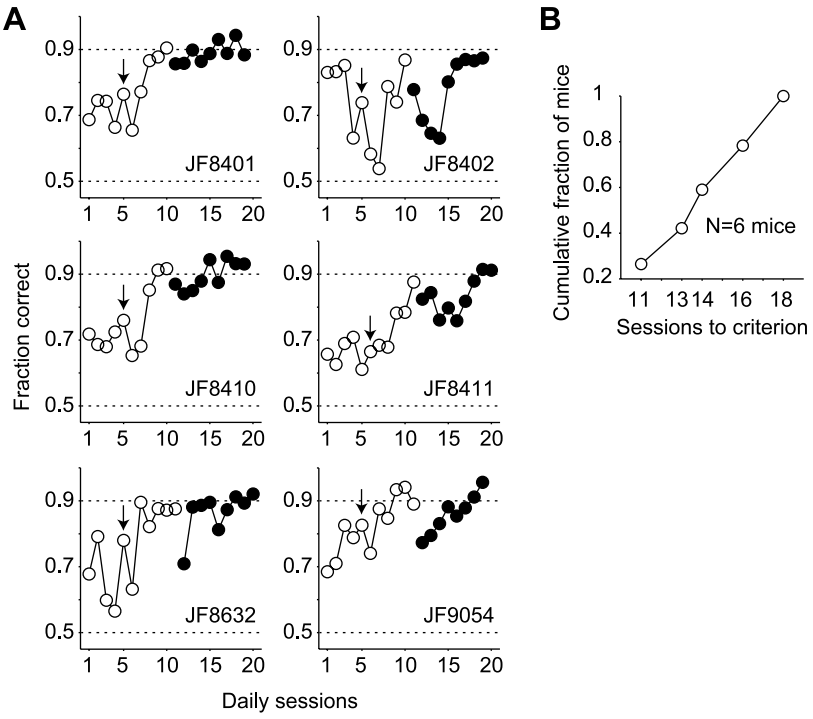

Supplementary Fig 3: Cortex aspiration lesion.

Contralateral to stimulus

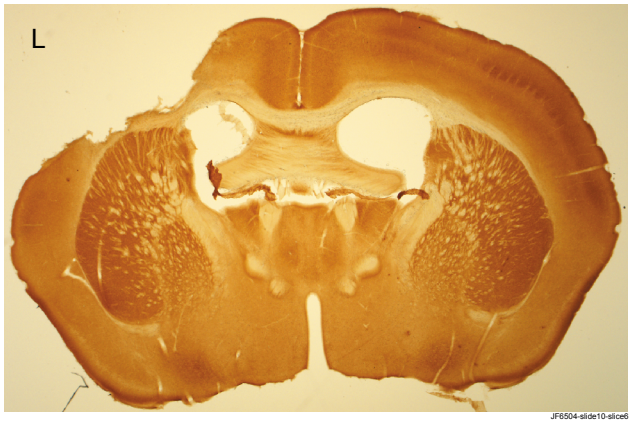


Ipsilateral to stimulus

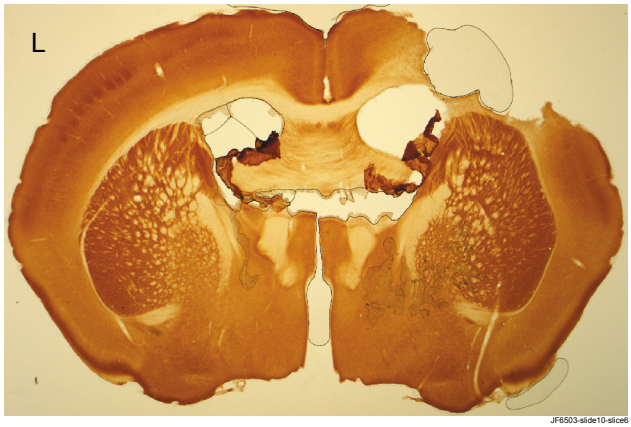

Supplementary Fig 4: Order of sessions for psychometric curve experiments.

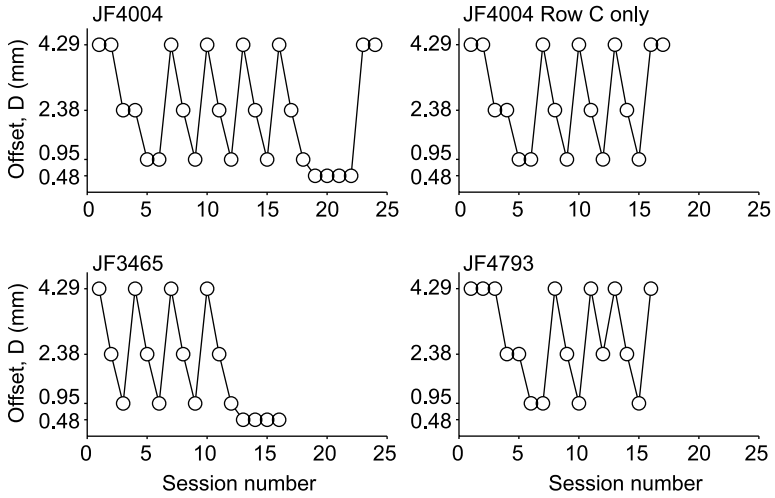

Supplementary Fig 5: Examples of whisking search strategies for multiple consecutive trials.

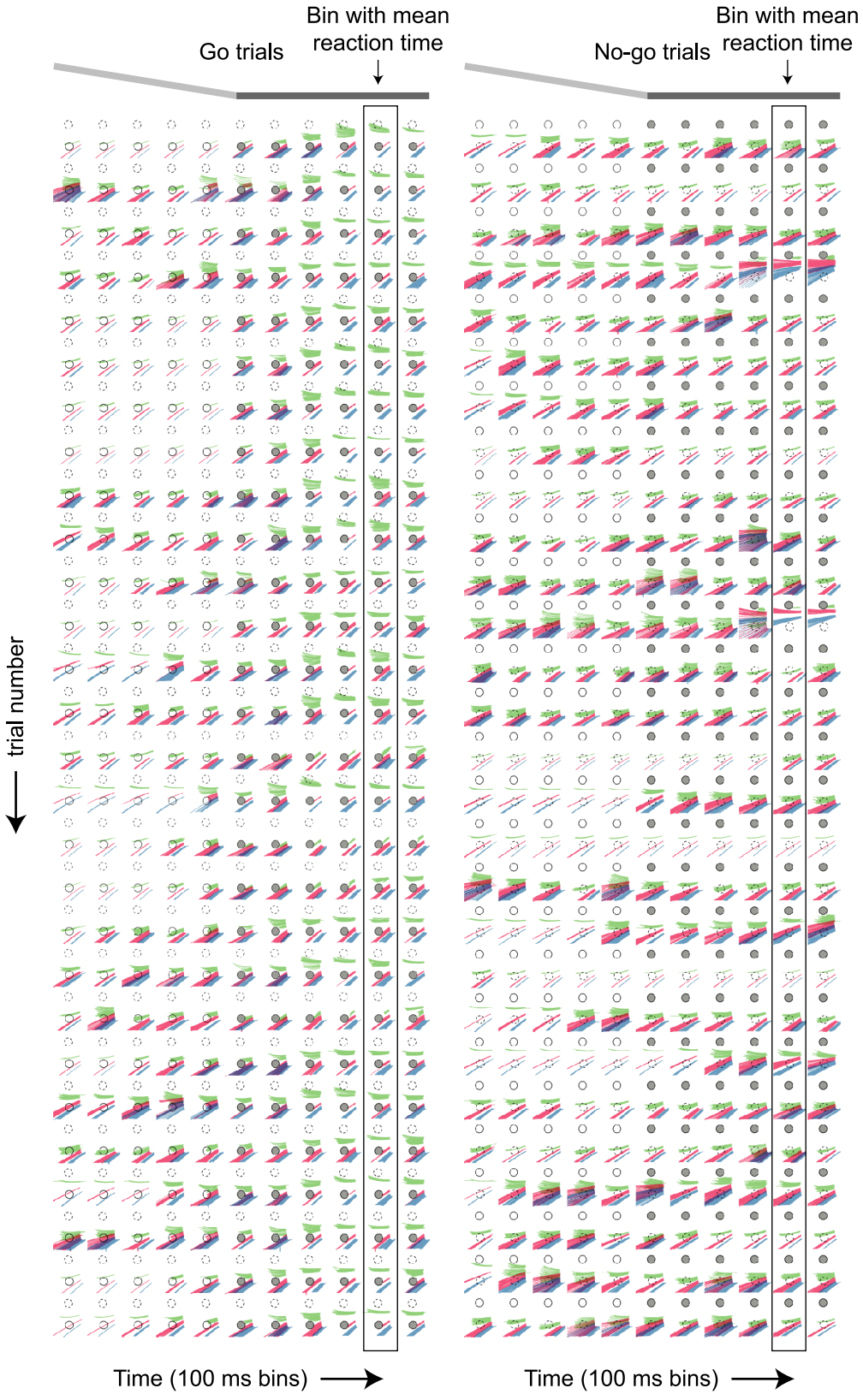

Supplementary Fig 6: Examples of high-velocity whisker movements.